LEARNING WHERE THE PHYSICS IS: PROBABILISTIC ADAPTIVE SAMPLING FOR STIFF PDES

Akshay Govind Srinivasan, Balaji Srinivasan
Indian Institute of Technology, Madras
Chennai, TN 600107, India
me22b102@smail.iitm.ac.in, sbalaji@dsai.iitm.ac.in

ABSTRACT

Modeling stiff partial differential equations (PDEs) with sharp gradients remains a significant challenge for scientific machine learning. While Physics-Informed Neural Networks (PINNs) struggle with spectral bias and slow training times, Physics-Informed Extreme Learning Machines (PIELMs) offer a rapid, closed-form linear solution but are fundamentally limited by physics-agnostic, random initialization. We introduce the Gaussian Mixture Model Adaptive PIELM (GMM-PIELM), a probabilistic framework that learns a probability density function representing the "location of physics" for adaptively sampling kernels of PIELMs. By employing a weighted EM algorithm, GMM-PIELM autonomously concentrates radial basis function centers in regions of high numerical error, such as shock fronts and boundary layers. This approach dynamically improves the conditioning of the hidden layer without the expensive gradient-based optimization(of PINNs) or Bayesian search. We evaluate our methodology on 1D singularly perturbed convection-diffusion equations with diffusion coefficients $\nu = 10^{-4}$. Our method achieves L_2 errors up to 7 orders of magnitude lower than baseline RBF-PIELMs, successfully resolving exponentially thin boundary layers while retaining the orders-of-magnitude speed advantage of the ELM architecture.

1 INTRODUCTION

Modeling stiff ODEs/PDEs with sharp gradients poses severe resolution challenges (Madhavi et al., 2025). While high-fidelity classical methods exist, they are often cost-prohibitive due to stability constraints and complex meshing requirements (Yagawa & Okuda, 2011). This motivates the development of mesh-free, model-based solvers to efficiently resolve stiff dynamics. Physics-Informed Neural Networks (PINNs) (Raissi et al., 2019) offer a versatile mesh-free framework but suffer from slow training and hyperparameter sensitivity. Recent benchmarks indicate they often require significantly more wall-clock time than classical solvers to reach comparable accuracy, particularly for stiff PDEs (McGreivy & Hakim, 2024; Karnakov et al., 2024). Furthermore, spectral bias and optimization pathologies frequently lead to the under-resolution of sharp gradients, even in overparameterized networks (Krishnapriyan et al., 2021)

Physics-Informed Extreme Learning Machines (PIELMs) (Dwivedi & Srinivasan, 2020) substitute iterative backpropagation with a closed-form linear least-squares solution, achieving orders-of-magnitude acceleration. Yet, the efficacy of PIELMs is fundamentally limited by their initialization: random, physics-agnostic hidden features often suffer from spectral mismatch with the underlying stiff dynamics, leading to ill-conditioned representations (Huang et al., 2006; Dwivedi et al., 2025b). Although Radial Basis Function variants like RBF-PIELMs (Dwivedi et al., 2025a; Srinivasan et al., 2025) introduce interpretable, localized receptivity, they typically rely on static node allocations that lack the flexibility to track evolving discontinuities and require manually designed problem-specific heuristics. Consequently, there remains a critical need for principled, data-driven adaptation mechanisms that can dynamically align basis functions with the moving wavefronts of singular perturbation problems while retaining the computational efficiency of linear solvers.

To tackle these challenges, this work introduces the **Gaussian Mixture Model Adaptive PIELM (GMM-PIELM)**, a probabilistic training framework that treats the PDE residual field as an error density over the computational domain. We postulate that the $\log(1 + |\text{residual}|)$ field can be interpreted as unnormalized probability density function representing the "location of physics". We then learn this distribution using an Expectation–Maximisation (E-M) based algorithm. GMM-PIELM concentrates hidden-unit centers in regions of high numerical error. This adaptive redistribution improves the conditioning of the hidden-layer system and enhances expressivity exactly where the solution exhibits stiff behavior, while retaining the linear least-squares solve of the ELM architecture (unlike Tang et al. (2023)). Compared to KAPI-ELM (Dwivedi et al., 2025b), that relies on iterative Bayesian optimization for center placement, our method relies on unsupervised learning of the probability density of the residual field. As demonstrated on 1D singularly perturbed convection–diffusion equations, the proposed method attains much lower L_2 errors than RBF-PIELM while capturing the complex boundary layer.

Contributions This paper presents a EM-based algorithm to adaptively sample kernels for PIELMs. Specifically:

- We present a fast and interpretable residual field based expectation maximization algorithm to adaptively sample kernels for solving stiff PDEs using RBF-PIELMs
- We evaluate the capability and efficiency of the algorithm against RBF-PIELMs using a 1D boundary layer problem with a single and double boundary layer as benchmark.

2 Mathematical Formulation

We consider a stationary PDE defined on a bounded domain $\Omega \subset \mathbb{R}^d$ with boundary $\partial\Omega$:

$$\mathcal{L}[u](x) = f(x), \quad x \in \Omega \quad \mathcal{B}[u](x) = g(x), \quad x \in \partial\Omega \tag{1}$$

where $\mathcal{L}$ is a linear differential operator, $\mathcal{B}$ is a boundary operator, $f(x)$ is a source term, and $g(x)$ is the boundary data. In RBF-PIELM, We approximate the solution $u(x)$ using a Single-Hidden-Layer Feedforward Network (SLFN) with N hidden neurons:

$$\hat{u}(x;\beta) = \sum_{j=1}^{N} \beta_j \phi_j(x) = \sum_{j=1}^{N} \beta_j \exp\left(-\frac{\|x - x_0^j\|^2}{2s_j^2}\right) \tag{2}$$

where β_j are the hidden unit weights and $\phi_j(x)$ are non-linear activations. x_0^j and s_j^2 are the parameters of RBF kernel. Sampling these points randomly poses challenge especially for stiff problems (refer Appendix Section A.1). Dwivedi et al. (2025a); Srinivasan et al. (2025) use a manually designed heuristic to sample these points. But these require prior knowledge of underlying physics and is challenging to adapt in dynamic problems.

2.1 GMM-PIELM: Gaussian Mixture Model-Based Kernel Adaptation

The accuracy of the approximation $\widehat{u}$ in the previous section is heavily contingent on the placement of the basis centers x_0^j and the choice of widths s_j, especially for stiff problems. We address this by proposing a probabilistic framework that allocates resources proportional to the local physical complexity of the problem.

Probabilistic Formulation Let $\mathcal{R}(x;\theta) = \mathcal{L}[\hat{u}_\theta](x) - f(x)$ denote the PDE residual field for the current approximation $\hat{u}_\theta$. Standard physics-informed approaches minimize the global L_2 norm of this residual, effectively averaging errors across the domain. However, for singularly perturbed problems, this global metric is dominated by smooth regions, often washing out the high-frequency errors localized at shocks or boundary layers (Krishnapriyan et al., 2021).

To address this, we postulate that the $\log(1 + |\text{residual}|)$ field acts as an unnormalized probability density function (PDF) representing the spatial concentration of approximation error. We provide justification for the choice of log-transform in Appendix Section A.5. We define the *Residual Energy Density*, $p_{\text{res}}(x)$, as:

$$p_{\text{res}}(x) = \frac{\log(1 + |\mathcal{R}(x;\theta)|)}{Z}, \quad \text{where} \quad Z = \int_\Omega \log(1 + |\mathcal{R}(z;\theta)|)\, dz. \tag{3}$$

Intuitively, $p_{\text{res}}(x)$ maps the "location of physics," highlighting regions where the spectral bandwidth is insufficient to capture the underlying dynamics (Nabian & Meidani, 2019; Wu et al., 2023).

GMM-PIELM Under this hypothesis, the optimal allocation of hidden neurons corresponds to a distribution of basis centers $\{\mathbf{c}_j\}_{j=1}^{N}$ that maximizes the likelihood of sampling from this residual landscape. Hence we model this distribution as a mixture of gaussian

$$x_0^j \sim p(x;\Theta) = \sum_{k=1}^{K} \pi_k \mathcal{N}(x \mid \mu_k, \Sigma_k), \tag{4}$$

where $\Theta = \{\pi_k, \mu_k, \Sigma_k\}_{k=1}^{K}$ are the mixing coefficients, means, and covariances, respectively. To fit this model to the evolving solution, we employ a weighted EM framework to maximize the residual-weighted log-likelihood. In the **E-step**, we evaluate the current approximation and compute the "responsibility" q_{ik}—the posterior probability that the i-th collocation point x_i (with residual weight $w_i = \log(1 + |\mathcal{R}(x_i)|)$) belongs to the k-th Gaussian component:

$$q_{ik} = \frac{\pi_k \mathcal{N}(x_i \mid \mu_k, \Sigma_k)}{\sum_{\ell=1}^{K} \pi_\ell \mathcal{N}(x_i \mid \mu_\ell, \Sigma_\ell)}. \tag{5}$$

In the subsequent **M-step**, we update the GMM parameters to concentrate the components in regions of high error. The updated means μ_k^* and covariances Σ_k^* are computed as:

$$N_k = \sum_{i=1}^{N_{eval}} w_i q_{ik}, \quad \mu_k^* = \frac{1}{N_k} \sum_{i=1}^{N_{eval}} w_i q_{ik} x_i, \quad \Sigma_k^* = \frac{1}{N_k} \sum_{i=1}^{N_{eval}} w_i q_{ik} (x_i - \mu_k^*)(x_i - \mu_k^*)^\top \tag{6}$$

where N_{eval} is the number of evaluation points on a dense grid. The derivation of the parameter updates is provided in Appendix Section A.4. Finally, we augment the adaptive sampling with a set of uniformly distributed centers to ensure global domain coverage and prevent basis depletion in low-residual regions. We then determine the local kernel width s_j based on the k-nearest neighbor distance to ensure consistent overlap even in highly clustered arrangements.

3 Numerical Experiments

We evaluate the capability of the GMM-PIELM framework against RBF-PIELM on the singularly perturbed 1D steady-state convection–diffusion equation with single and double boundary layers. It is a canonical benchmark for validating numerical schemes designed for stiff dynamics (Roos et al., 2008). The underlying PDE is defined on the domain $x \in (0, 1)$ as:

$$-\nu u_{xx} + u_x = 0 \tag{7}$$

where $\nu > 0$ represents the diffusion coefficient. The exact analytical solution is given in Dwivedi et al. (2025b). We assess performance in the stiff regimes of $\nu = 10^{-4}$. This equation serves as a fundamental model for high-Péclet-number transport phenomena encountered in fluid mechanics, isolating the physics of boundary layer formation where advective forces dominate diffusive ones.

The primary computational challenge in this regime is the formation of an exponentially thin boundary layer of width $\delta \sim \mathcal{O}(\nu)$ near the outlet ($x = 1$). Resolving this feature typically necessitates prohibitive mesh densities ($N \gg 1/\nu$) for uniform solvers, while learning-based methods like PINNs suffer from pronounced spectral bias, often failing to capture the high-frequency transition without specialized loss weighting (Krishnapriyan et al., 2021; Wang et al., 2022). Similarly, standard PIELMs with randomized initialization frequently lack sufficient basis support in this narrow region, leading to ill-conditioned linear systems and degraded accuracy (refer Appendix Section A.1). Refer Appendix Section A.6 for implementation details.

Results We observe from figures 1a and 1c that our method (GMM-PIELM) is able to capture the sharp boundary layer at $x = 1$ ($x = 0, 1$ in case of double boundary layer) as opposed to our baseline (RBF-PIELM). Our solution achieves upto 7 orders of magnitude better accuracy as compared to RBF-PIELM (refer Table 1). Additionally, we observe from figures 1b and 1d that the learned GMM distribution has similar structure to the error.

Boundary Condition	Method	Mean L_2 Error (RMSE)	Time (s)
Single ($N = 300$)	Baseline RBF-PIELM	5.00×10^{-1}	0.071
	Ours (GMM-adaptive)	2.73×10^{-8}	0.696
Double ($N = 500$)	Baseline RBF-PIELM	1.01×10^{-5}	0.312
	Ours (GMM-adaptive)	1.04×10^{-9}	1.776

Table 1: Comparison of Baseline vs. GMM-adaptive RBF-PIELM for single and double boundary layer problem ($\nu = 10^{-4}$), showcasing significant improvement in accuracy.

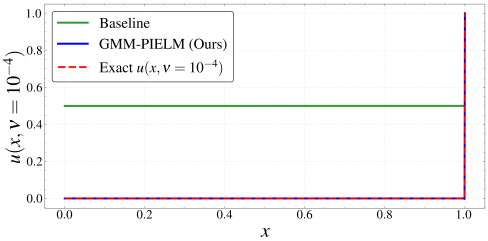

(a) Solution profile for single boundary layer

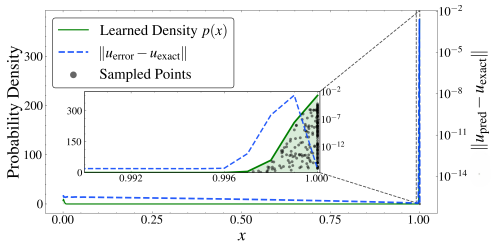

(b) Error density and learned distribution for single boundary layer

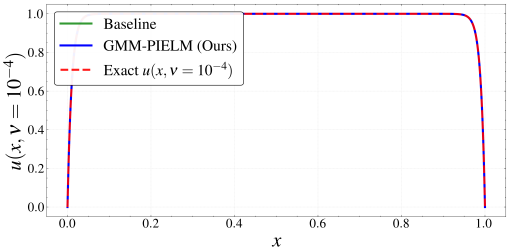

(c) Solution profile for double boundary layer

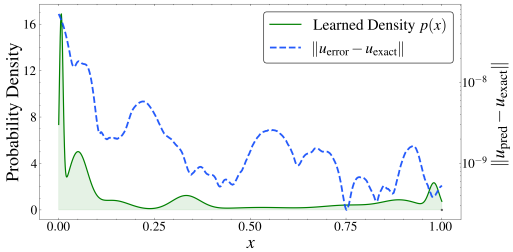

(d) Error density and learned distribution for double boundary layer

Figure 1: Performance analysis of GMM-PIELM on the 1D convection-diffusion equation with single and double boundary layer.

4 Conclusion

This work introduces the Gaussian Mixture Model Adaptive PIELM (GMM-PIELM), a framework that treats the PDE residual as a probability density representing the "location of physics." By interpreting the $\log(1+|\text{residual}|)$ field as an unnormalized PDF, we use an EM algorithm to dynamically concentrate hidden-unit centers and widths in regions of high numerical error. This approach addresses the fundamental initialization limitations of standard Physics-Informed Extreme Learning Machines; instead of relying on physics-agnostic random sampling or heuristic node placement, the algorithm tracks sharp gradients in solution automatically. Numerical experiments on 1D singularly perturbed convection–diffusion equations demonstrate that GMM-PIELM achieves L_2 errors up to 7 orders of magnitude lower than baseline RBF-PIELMs, successfully resolving thin boundary layers ($\nu = 10^{-4}$) that standard methods fail to capture. While the adaptive process incurs a moderate computational overhead, it retains the fundamental speed advantages of the ELM architecture over gradient-based training. Consequently, GMM-PIELM offers a highly efficient and robust alternative for solving stiff, multi-scale physical systems that typically defy traditional mesh-less methods.

Future Work Future Work will focus on extending this probabilistic framework to time-dependent PDEs, allowing the GMM centroids to track moving wavefronts in real-time. Additionally, we aim to investigate the scalability and stability of this approach to high-dimensional problems and complex geometries to enable it's use across multitude of applications.

REFERENCES

Vikas Dwivedi and Balaji Srinivasan. Physics informed extreme learning machine (PIELM) – a rapid method for the numerical solution of partial differential equations. *Neurocomputing*, 391: 96–118, 2020. doi: 10.1016/j.neucom.2019.12.099.

Vikas Dwivedi, Bruno Sixou, and Monica Sigovan. Curriculum learning-driven PIELMs for fluid flow simulations. *Neurocomputing*, 616:130924, 2025a. doi: 10.1016/j.neucom.2024.130924.

Vikas Dwivedi, Balaji Srinivasan, et al. Kernel-adaptive PI-ELMs for forward and inverse problems in PDEs with sharp gradients. *arXiv preprint arXiv:2507.10241*, 2025b.

Guang-Bin Huang, Qin-Yu Zhu, and Chee-Kheong Siew. Extreme learning machine: Theory and applications. *Neurocomputing*, 70:489–501, 2006. doi: 10.1016/j.neucom.2005.12.126.

Petr Karnakov, Sergey Litvinov, and Petros Koumoutsakos. Solving inverse problems in physics by optimizing a discrete loss: Fast and accurate learning without neural networks. *PNAS Nexus*, 3 (1):pgae005, 2024. doi: 10.1093/pnasnexus/pgae005.

Aditi Krishnapriyan, Amir Gholami, Shandian Zhe, Robert Kirby, and Michael W. Mahoney. Characterizing possible failure modes in physics-informed neural networks. In *Advances in Neural Information Processing Systems*, volume 34, pp. 26548–26560, 2021.

M. V. D. N. S. Madhavi, Mir Sohail Ali, Satyawan L. Dhondge, Vijay Narayan Deshmukh, Gajendra R. Gandhe, and P. V. S. Sairam. Advanced numerical methods for solving nonlinear partial differential equations in fluid mechanics: Applications in aerospace engineering. *International Journal of Applied Mathematics*, 38(3s), 2025. URL https://ijamjournal.org/ijam/publication/index.php/ijam/article/view/135.

Nick McGreivy and Ammar Hakim. Weak baselines and reporting biases lead to overoptimism in machine learning for fluid-related partial differential equations. *Nature Machine Intelligence*, 6(10):1256–1269, 2024. URL https://www.nature.com/articles/s42256-024-00897-5.

Mohammad Amin Nabian and Rael Meidani. Efficient training of physics-informed neural networks via adaptive importance sampling. *Computer-Aided Civil and Infrastructure Engineering*, 34(12): 1026–1037, 2019.

Maziar Raissi, Paris Perdikaris, and George E. Karniadakis. Physics-informed neural networks: A deep learning framework for solving forward and inverse problems involving nonlinear partial differential equations. *Journal of Computational Physics*, 378:686–707, 2019. doi: 10.1016/j.jcp.2018.10.045.

Hans-Görg Roos, Martin Stynes, and Lutz Tobiska. *Robust Numerical Methods for Singularly Perturbed Differential Equations: Convection-Diffusion-Reaction and Flow Problems*, volume 24 of *Springer Series in Computational Mathematics*. Springer-Verlag, Berlin, Heidelberg, 2nd edition, 2008. doi: 10.1007/978-3-540-34467-4.

Akshay Govind Srinivasan, Vikas Dwivedi, and Balaji Srinivasan. Deep vs. shallow: Benchmarking physics-informed neural architectures on the biharmonic equation. *arXiv preprint arXiv:2510.04490*, 2025.

Kejun Tang, Xiaoliang Wan, and Chao Yang. Das-pinns: A deep adaptive sampling method for solving high-dimensional partial differential equations. *Journal of Computational Physics*, 476: 111868, 2023. ISSN 0021-9991. doi: https://doi.org/10.1016/j.jcp.2022.111868. URL https://www.sciencedirect.com/science/article/pii/S0021999122009317.

Sifan Wang, Xinling Yu, and Paris Perdikaris. When and why PINNs fail to train: A neural tangent kernel perspective. *Journal of Computational Physics*, 449:110768, 2022.

Chuizheng Wu, Min Zhu, Qiquan Tan, Yogesh Ktha, and E. Lu. A comprehensive review of physics-informed neural networks: Perspectives on the failure modes and solution strategies. *arXiv preprint arXiv:2303.08823*, 2023.

Genki Yagawa and Hiroshi Okuda. Computational performance of free mesh method applied to continuum mechanics problems. *Interaction and Multiscale Mechanics*, 4(1):1–28, 2011. doi: 10.12989/imm.2011.4.1.001.

A APPENDIX

A.1 THE CONDITION NUMBER PROBLEM

To determine $\beta = [\beta_1, \ldots, \beta_L]^T$, we substitute the ansatz $\hat{u}$ into the PDE and boundary conditions and evaluate them at a set of collocation points. Let $\{x_f^{(i)}\}_{i=1}^{N_f}$ be interior points and $\{x_b^{(k)}\}_{k=1}^{N_b}$ be boundary points.

For a linear operator $\mathcal{L}$, the residual constraints are linear in β:

$$\sum_{j=1}^{L} \beta_j \mathcal{L}[\phi_j](x_f^{(i)}) = f(x_f^{(i)}) \tag{8}$$

$$\sum_{j=1}^{L} \beta_j \mathcal{B}[\phi_j](x_b^{(k)}) = g(x_b^{(k)}) \tag{9}$$

This system can be written in matrix form as $\mathbf{H}\beta = \mathbf{T}$, where:

$$\mathbf{H} = \begin{bmatrix} \mathcal{L}[\phi_1](x_f^{(1)}) & \ldots & \mathcal{L}[\phi_L](x_f^{(1)}) \\ \vdots & \ddots & \vdots \\ \mathcal{L}[\phi_1](x_f^{(N_f)}) & \ldots & \mathcal{L}[\phi_L](x_f^{(N_f)}) \\ \lambda\mathcal{B}[\phi_1](x_b^{(1)}) & \ldots & \lambda\mathcal{B}[\phi_L](x_b^{(1)}) \\ \vdots & \ddots & \vdots \end{bmatrix}, \quad \mathbf{T} = \begin{bmatrix} f(x_f^{(1)}) \\ \vdots \\ f(x_f^{(N_f)}) \\ \lambda g(x_b^{(1)}) \\ \vdots \end{bmatrix} \tag{10}$$

Here, λ is a penalty weight for boundary conditions. Since usually $N_f + N_b > L$, the system is overdetermined. The optimal weights in the least-squares sense are obtained via the Moore-Penrose pseudo-inverse:

$$\beta^* = \mathbf{H}^\dagger \mathbf{T} = (\mathbf{H}^T\mathbf{H})^{-1}\mathbf{H}^T\mathbf{T} \tag{11}$$

The accuracy of the least-squares solution depends heavily on the condition number $\kappa(\mathbf{H})$. In stiff PDEs, if the collocation points are uniformly distributed, the rows of $\mathbf{H}$ corresponding to the smooth regions are well-behaved, but the rows corresponding to the boundary layer (where gradients are huge) are sparse. If only a few points fall into the layer, the matrix $\mathbf{H}$ fails to capture the high-frequency dynamics, essentially treating the layer as noise. This results in a poor approximation β^* that smooths over the shock. To fix this, we must increase the row density in the shock region, thereby explicitly constraining the solver to respect the physics in that zone.

A.2 ALGORITHMIC IMPLEMENTATION

This probabilistic feedback loop is formalized in Algorithm 1. The procedure alternates between a fast linear solve (ELM step) and a statistical adaptation of the basis functions (EM step) until the residual energy stabilizes.

Algorithm 1 GMM-PIELM Adaptive Solving

Require: Operators $\mathcal{L}, \mathcal{B}$; Iterations T; Mixing Ratio α
Initialize: Centers $x_0^{(0)}$ (uniform), Widths $s_j^{(0)}$ (constant)
for $t = 0$ to T **do**
  // Step 1: Linear Solve (PIELM)
  Construct matrices $H^{\text{in}}, H^{\text{bd}}$ using current $\{x_0^j, s_j\}$
  Solve $\mathbf{w}^{(t)} = \arg\min_{\mathbf{w}} \|H\mathbf{w} - \mathbf{b}\|_2^2$
  Construct approx: $\widehat{u}^{(t)}(x) = \sum w_j \phi(x; x_0^j, s_j)$
  // Step 2: Assessment
  Evaluate residual $\mathcal{R}(x;\theta) = \mathcal{L}[\widehat{u}^{(t)}] - f$ on grid
  Compute density $p_{\text{res}}(x) \propto \log(1 + |\mathcal{R}(x;\theta)|)$
  if $t < T$ **then**
    // Step 3: Adaptation (EM & Hybrid Sampling)
    Fit GMM parameters Θ to samples from $p_{\text{res}}(x)$
    Sample $x_{\text{gmm}} \sim p(x;\Theta)$ and $x_{\text{uni}} \sim \mathcal{U}(\Omega)$
    Update centers: $x_0^{(t+1)} \leftarrow \alpha x_{\text{gmm}} \cup (1-\alpha) x_{\text{uni}}$
    Update widths: $s_j^{(t+1)} \leftarrow \beta \cdot \text{dist}_k(x_0^j) + \epsilon$
  end if
end for
Return Final approximation $\widehat{u}^{(T)}$

A.3 Compute Specifications

For Experiments, we run the experiment only on a CPU namely, a Ryzen 7 5800H with 16GB RAM. All processes are run on a single thread and process.

A.4 Derivation of EM Steps

The objective of the GMM-PIELM framework is to adaptively distribute the centers of the radial basis functions to match the spatial distribution of the PDE error. We postulate that the squared PDE residual field represents an unnormalized probability density function (PDF) indicating the "location of physics."

Let the **Residual Energy Density**, $p_{res}(x)$, be defined as:

$$p_{\text{res}}(x) = \frac{\log(1 + |\mathcal{R}(x;\theta)|)}{Z}, \quad \text{where} \quad Z = \int_\Omega \log(1 + |\mathcal{R}(z;\theta)|)\, dz. \tag{12}$$

We approximate this target distribution using a Gaussian Mixture Model (GMM), $p(x;\Theta)$, parameterized by $\Theta = \{\pi_k, \mu_k, \Sigma_k\}_{k=1}^K$:

$$p(x;\Theta) = \sum_{k=1}^{K} \pi_k \mathcal{N}(x|\mu_k, \Sigma_k) \tag{13}$$

We seek the parameters Θ that make the model distribution $p(x;\Theta)$ best approximate the target residual distribution $p_{res}(x)$. The information-theoretic measure of the difference between two probability distributions is the **Kullback-Leibler (KL) Divergence**.

We minimize the KL divergence from the true distribution p_{res} to the model p_Θ:

$$\Theta^* = \arg\min_\Theta D_{KL}(p_{res} || p_\Theta) \tag{14}$$

$$= \arg\min_\Theta \int_\Omega p_{res}(x) \ln\left(\frac{p_{res}(x)}{p(x;\Theta)}\right) dx \tag{15}$$

$$= \arg\min_\Theta \left[\int_\Omega p_{res}(x) \ln p_{res}(x) dx - \int_\Omega p_{res}(x) \ln p(x;\Theta) dx\right] \tag{16}$$

The first term represents the entropy of the residual field. Since the residual $\mathcal{R}(x)$ is fixed during the adaptation step (it depends only on the previous iteration's weights), this term is constant with respect to Θ. Minimizing the KL divergence is therefore equivalent to maximizing the second term (the cross-entropy):

$$\Theta^* = \arg\max_{\Theta} \int_{\Omega} p_{res}(x) \ln p(x;\Theta) dx \tag{17}$$

We approximate the integral using a dense set of collocation points $\{x_i\}_{i=1}^N$ via a Riemann sum. Substituting $p_{res}(x_i) \propto \log(1 + |\mathcal{R}(x_i)|)$:

$$\Theta^* \approx \arg\max_{\Theta} \sum_{i=1}^{N} \log(1 + |\mathcal{R}(x_i)|) \ln p(x_i;\Theta) \tag{18}$$

Defining the weight $w_i = \log(1 + |\mathcal{R}(x_i)|)$, we arrive at the **Weighted Log-Likelihood** objective function:

$$\mathcal{L}(\Theta) = \sum_{i=1}^{N} w_i \ln \left(\sum_{k=1}^{K} \pi_k \mathcal{N}(x_i|\mu_k, \Sigma_k) \right) \tag{19}$$

Direct maximization of $\mathcal{L}(\Theta)$ is intractable due to the summation inside the logarithm. We employ the EM algorithm. We introduce latent variables $z_i \in \{1, \dots, K\}$ indicating the component assignment for point x_i.

The expected complete-data log-likelihood (the Q-function) for the weighted dataset is:

$$Q(\Theta, \Theta^{(t)}) = \sum_{i=1}^{N} w_i \sum_{k=1}^{K} q_{ik} \left[\ln \pi_k + \ln \mathcal{N}(x_i|\mu_k, \Sigma_k) \right] \tag{20}$$

where $q_{ik} = P(z_i = k|x_i, \Theta^{(t)})$ is the responsibility computed in the E-step (Eq. 5 in the paper).

We maximize Q with respect to μ_k and Σ_k by setting the gradients to zero.

Consider the terms in Q dependent on μ_k:

$$J(\mu_k) = \sum_{i=1}^{N} w_i q_{ik} \left(-\frac{1}{2}(x_i - \mu_k)^T \Sigma_k^{-1} (x_i - \mu_k) \right) \tag{21}$$

Taking the derivative with respect to μ_k:

$$\frac{\partial J}{\partial \mu_k} = \sum_{i=1}^{N} w_i q_{ik} \Sigma_k^{-1} (x_i - \mu_k) \tag{22}$$

Setting $\frac{\partial J}{\partial \mu_k} = 0$ and multiplying by Σ_k:

$$\sum_{i=1}^{N} w_i q_{ik} (x_i - \mu_k) = 0 \tag{23}$$

$$\sum_{i=1}^{N} w_i q_{ik} x_i = \mu_k \sum_{i=1}^{N} w_i q_{ik} \tag{24}$$

Solving for μ_k:

$$\boxed{\mu_k^* = \frac{\sum_{i=1}^{N} w_i q_{ik} x_i}{\sum_{i=1}^{N} w_i q_{ik}}} \tag{25}$$

Consider the terms dependent on Σ_k:

$$J(\Sigma_k) = \sum_{i=1}^{N} w_i q_{ik} \left(-\frac{1}{2} \ln |\Sigma_k| - \frac{1}{2}(x_i - \mu_k)^T \Sigma_k^{-1} (x_i - \mu_k) \right) \tag{26}$$

Using the matrix derivative identities $\frac{\partial \ln|\Sigma|}{\partial \Sigma} = \Sigma^{-1}$ and $\frac{\partial a^T \Sigma^{-1} a}{\partial \Sigma} = -\Sigma^{-1} a a^T \Sigma^{-1}$:

$$\frac{\partial J}{\partial \Sigma_k} = \sum_{i=1}^{N} w_i q_{ik} \left(-\frac{1}{2}\Sigma_k^{-1} + \frac{1}{2}\Sigma_k^{-1}(x_i - \mu_k)(x_i - \mu_k)^T \Sigma_k^{-1} \right) \tag{27}$$

Setting to zero and multiplying by Σ_k on both sides:

$$\sum_{i=1}^{N} w_i q_{ik} I = \sum_{i=1}^{N} w_i q_{ik}(x_i - \mu_k)(x_i - \mu_k)^T \Sigma_k^{-1} \tag{28}$$

$$\Sigma_k \left(\sum_{i=1}^{N} w_i q_{ik} \right) = \sum_{i=1}^{N} w_i q_{ik}(x_i - \mu_k)(x_i - \mu_k)^T \tag{29}$$

Solving for Σ_k:

$$\boxed{\Sigma_k^* = \frac{\sum_{i=1}^{N} w_i q_{ik}(x_i - \mu_k^*)(x_i - \mu_k^*)^T}{\sum_{i=1}^{N} w_i q_{ik}}} \tag{30}$$

These equations exactly match Equation 6 in the GMM-PIELM paper formulation.

A.5 Justification on log-transform

$p_{res}(x) \propto \log(1 + |\mathcal{R}(x)|)$ is a critical mechanism for dynamic range compression, particularly in the stiff regimes targeted by our framework. Empirical tests using the raw squared residual field as the density concentrated the all the centers at the boundary, since the residuals in singularly perturbed problems vary by several orders of magnitude between the boundary layer and the rest of the domain. This led to a "collapse" of the basis distribution where global domain information was lost and the linear system became ill-conditioned in smoother regions. By applying the $\log$ transform, we successfully damp these extreme variations, allowing the Gaussian Mixture Model to resolve the "shoulders" of the error distribution rather than just the singularity. This ensures that while high-gradient regions are prioritized, sufficient information and basis support are maintained across the entire domain to yield a stable and accurate solution.

A.6 Implementation Details

Experimental Setup All experiments were implemented using `scikit-learn` for GMM estimation and `scipy` for linear algebra operations, with a fixed random seed of 42. For both single and double boundary layer experiments, we sample a fixed set of $N_{\text{eval}} = 1500$ collocation points uniformly from the domain $\Omega = (0, 1)$ to construct the linear system. Boundary conditions are enforced via soft constraints by appending the boundary coordinates to the collocation set.

Baseline RBF-PIELM The baseline model initializes the hidden layer with N neurons ($N = 300$ for single, $N = 500$ for double boundary layers). The centers are sampled uniformly:

$$x_0^j \sim \text{Uniform}(0, 1), \quad j = 1, \ldots, N. \tag{31}$$

The widths are set to a constant value $s_j = \frac{|\Omega|}{N} \times 2.5$, consistent with the overlap analogy presented in Dwivedi et al. (2025a).

Proposed: Adaptive GMM-PIELM The adaptive method refines the network architecture over T iterations. In each iteration, we compute the residual field $\mathcal{R}(x; \theta)$ on the dense grid and construct the residual energy density $p_{\text{res}}(x)$ as defined in Eq. equation 12. We then fit a GMM to data sampled from $p_{\text{res}}(x)$ and generate a new set of centers $\{x_0^j\}_{j=1}^N$ using a *hybrid sampling strategy*:

- **Residual-Guided** (100α**%):** Sampled from the fitted GMM components to target high-error regions (boundary layers).
- **Global Uniform** ($100(1-\alpha)$**%):** Sampled uniformly from Ω to act as a safety net against basis depletion in smooth regions.

To accommodate the non-uniform clustering of centers, the local widths s_j are adapted using k-Nearest Neighbors (k-NN):

$$s_j = \beta \cdot \text{dist}_k(x_0^j) + \epsilon, \tag{32}$$

where dist_k is the Euclidean distance to the k-th neighbor ($k = 2$) and β is an overlap scaling factor.

Hyperparameters Table 2 details the specific parameters used for the Single Boundary Layer (BL) and Double BL experiments.

Table 2: Hyperparameter settings for implementation.

Parameter	**Single BL**	**Double BL**
Diffusivity (ν)	10^{-4}	10^{-4}
Number of Neurons (N)	300	500
GMM Components (K)	8	16
Hybrid Ratio (α)	0.7	0.7
Adaptation Iterations (T)	3	3
Sigma Scaling (β)	1.1	1.5
Random Seed	42	42